
Eliciting associations between clinical variables from LLMs via comparison questions across populations

Fabian Kabus¹, Kian Kordtomeikel², Thomas Brox², Heinz Wiendl⁴,
Daiana Stolz³, Harald Binder¹

¹Institute of Medical Biometry and Statistics (IMBI), Medical Center, University of Freiburg

²Department of Computer Science, Faculty of Engineering, University of Freiburg

³Department of Pneumology, Medical Center, University of Freiburg

⁴Department of Neurology and Neurophysiology, Medical Center, University of Freiburg

fabian.kabus@uniklinik-freiburg.de

Abstract

The training data of large language models (LLMs) comprises a wide range of biomedical literature, reflecting data from many different patient populations. We investigate how it might be possible to recover information on correlation and causal links between patient characteristics, as a key building block for medical decision making. To avoid the pitfalls of direct elicitation, we propose an approach based on structured comparison questions, specifically patient comparison triplet questions. This is combined with a statistical model for the LLM representation that provides estimates of correlations without access to activations or model internals. Intuitively, we consider how similarity decisions of LLMs based on a first variable are affected by providing information on a second variable for one of the patients being assessed. We then induce prompt-level environment shifts to obtain correlation estimates for different subpopulations, which enables an invariant causal prediction (ICP) approach to obtain conservative candidate parent links. We demonstrate the method in two clinical domains, chronic obstructive pulmonary disease (COPD) and multiple sclerosis (MS). Across prompted environments, the elicited correlations are smooth, stable, and clinically interpretable, yet vary in a statistically significant way that supports downstream invariance testing, such that ICP provides a small set of candidate invariant parent links. These results show that indirect elicitation via triplet comparisons can recover meaningful association structure from LLMs and offer a cautious route from implicit correlations to causal statements that are congruent with LLM answering patterns.

1 Introduction

As large language models (LLMs) are becoming a viable option for clinical decision tasks [Brodeur et al., 2026], a major question is how to best query LLMs, and how the representation of clinical settings by LLMs could be formalized. We focus on the task of assessing the association between different patient characteristics, via correlation or causal links, as a key ingredient of clinical decisions. As LLMs have been trained on a multitude of biomedical papers describing a broad range of different patient populations, it might be feasible to not only obtain a general statement, e.g. on the correlation of two clinical markers, but values specific to a decision task and subpopulation at hand, by getting the LLM to give more weight to relevant evidence. An obvious approach for retrieving such information is to ask directly: "What is the correlation between X and Y in population Z?" Direct queries, however, may fail in multiple ways. First, the answer may reflect recall of a specific statement rather than aggregated knowledge across studies. Second, even when the model responds with a plausible number, we cannot verify whether it respects that relationship when subsequently

used for decision-making. Beyond these fundamental issues, models exhibit sycophancy by adjusting answers to match perceived user beliefs [Sharma et al., 2024], responses are sensitive to the order of options [Pezeshkpour and Hruschka, 2024], outputs may be hallucinated without grounding [Ji et al., 2023], and chain-of-thought explanations can reflect post-hoc rationalization rather than actual computation [Lindsey et al., 2025]. This implies that when extracting LLM knowledge, we should treat LLMs as experimental subjects to be measured, not as self-reflecting agents to be asked.

The cognitive sciences have faced similar challenges when investigating the representations of human subjects, and have developed approaches for obtaining quantitative representations from structured comparison questions [Suppes et al., 1989]. Inspired by this research, we specifically propose to query LLMs with triplet questions—“Is entity 3 more similar to entity 1 or to entity 2?”—to obtain implicit correlations between patient characteristics, and to formalize the problem representation of LLMs. This also is related to more recent results, where triplet questions have been used to recover similarity structure [Vankadara et al., 2023] and applied to derive clinical concept embeddings from LLMs [Kabus et al., 2026].

To obtain information about the relationship between two patient characteristics, i.e. variables, we construct a triplet question involving three artificial patients, denoted 1, 2, and 3. We specify the values of the first variable for all three patients, but a value for the second variable is specified only for patient 3. This allows us to observe whether the value of the second variable tips the balance of the LLM similarity assessment of patient 3. By systematically varying the values, we can then assess how extreme the values of the second variable have to be to influence the decision, which carries information on correlation. We formalize this intuition into a statistical surrogate model for the LLM representation and decision to obtain estimates of implied correlation coefficients, including confidence intervals. We demonstrate the method in two clinical settings, with lung function markers in chronic obstructive pulmonary disease (COPD) and multiple sclerosis (MS) biomarkers, highlighting how different correlation estimates are obtained for different patient populations, contrasted with results from directly requesting correlation values from LLMs.

Having access to estimated correlations from different subpopulations is also useful for causal assessment. Specifically, Invariant Causal Prediction [ICP; Peters et al., 2016] allows us to test for causal links when given observational data from multiple environments, such as patient populations, that share the same causal structure. The invariance principle is as follows: if X causally affects Y , then the conditional distribution $P(Y | X)$, e.g. as assessed by regression models, remains stable across environments, even as the marginal distribution of X shifts. Spurious correlations, by contrast, break under distribution shift. The original ICP approach requires several individual-level datasets from different patient populations, but these might be difficult to obtain in practice. We demonstrate how the required regression parameter estimates can alternatively be obtained from our proposed correlation estimations, including uncertainty to enable statistical testing. To implement this, we synthesize environments through prompt variations, preceding the triplet question, by specifying the mean of the variable in the subpopulation under consideration. This allows us to identify causal relationships that congruently describe LLM decision behavior.

Our contributions are as follows:

- **Triplet-based extraction of clinical associations.** We introduce a framework that recovers pairwise correlations from LLM similarity judgments without access to model internals.
- **Prompted environments for causal assessment.** We estimate environment-specific correlations in prompted subpopulations and use ICP to obtain candidate parent links.
- **Clinical demonstration in COPD and MS.** We show that the extracted associations are clinically interpretable, more stable than direct correlation queries, and support a small set of plausible invariant parent links.

Empirically, triplet decision surfaces are smooth and well fit by the surrogate model, and triplet-based correlation estimates are substantially less noisy than direct numeric queries. The implied correlations are clinically plausible and generally align known characteristics. Further, across prompted environments, ICP identifies a small conservative set of invariant parent links.

Section 2 introduces the triplet representation and decision model, derives the symmetric correlation estimator, and describes the uncertainty-aware ICP procedure with prompted environment shifts. Section 3 describes the clinical applications and experimental protocol, Section 4 reports the empirical results, Section 5 discusses related work, and Section 6 provides concluding remarks.

2 Methods

Our method treats the LLM as an experimental subject from which information on the association between different variables, e.g., different patient characteristics, is to be obtained. The basic building block is the elicitation of correlation for pairs of variables. For each variable pair, we ask patient comparison triplet questions, fit a surrogate model to the resulting binary choices, and recover the model’s implied correlation from the fitted slopes. Repeating this procedure for different prompted environments (i.e. patient subpopulations) yields correlation matrices that we pass to invariant causal prediction.

2.1 Triplet questions

Let $\mathcal{X} = \{X_1, \dots, X_p\}$ denote the variable set of interest. To extract pairwise correlation structure, we query the LLM about three patients, Patient 1, 2, and 3, and pairs of variables X_j and X_k , $j \neq k$. All experiments are replicated across distinct environments $e \in \{1, \dots, m\}$, where each environment has its own implied population means $\mu^{(e)} = (\mathbb{E}_e[X_1], \dots, \mathbb{E}_e[X_p])$, and is implemented via a corresponding prompt text. Variation in these means serves as a synthetic distribution shift for the downstream ICP analysis.

For a fixed environment e , X_j is reported for all three patients, i.e. the question specifies values $X_j^{(1)}, X_j^{(2)}, X_j^{(3)}$. The value of the other variable $X_k^{(3)}$ is specified only for Patient 3. The LLM is asked whether Patient 3 is more similar to Patient 1 or to Patient 2, taking $X_k^{(3)}$ into account. The binary response $Y_{jk}^{(e)} \in \{1, 2\}$ is our observation for subsequent modeling. We collect responses per environment by varying $(X_j^{(3)}, X_k^{(3)})$ over a regular grid while holding $(X_j^{(1)}, X_j^{(2)})$ fixed. If the representation of the LLM entails a strong relation between X_j and X_k , presentation of a specific value $X_k^{(3)}$ in relation to the values $X_j^{(1)}, X_j^{(2)}, X_j^{(3)}$ intuitively should more strongly influence the answer. We also consider a version of the questions, where the roles of X_j and X_k are flipped. The symmetric estimator of the correlation in Section 2.3 integrates LLM answers from both versions.

2.2 Decision surrogate model based on a rational LLM representation

For inferring a correlation from triplet question answers, we assume an LLM representation that reflects rational behavior. Specifically, the value $X_j^{(3)}$ is assumed to be a noisy measurement of the true state $X_j^{*,(3)}$ of Patient 3, i.e. $X_j^{(3)} = X_j^{*,(3)} + \epsilon_j$, with $\mathbb{E}(\epsilon_j) = 0$ and $\text{Var}(\epsilon_j) = \sigma_j^2$. The additionally specified value $X_k^{(3)}$ then provides a second route towards $X_j^{*,(3)}$. We assume a linear relation $X_j^* = a_0 + a_1 X_k + U_{j|k}$, where $U_{j|k} \perp X_k$ with variance $\tau_{j|k}^2$. Letting $s_j^2 = \text{Var}(X_j)$ and $s_k^2 = \text{Var}(X_k)$, the slope is directly related to the population correlation ρ_{jk} via

$$a_1 = \rho_{jk} s_j / s_k. \quad (1)$$

Assuming the LLM representation entails a measurement error perspective, the LLM prediction would incorporate the projection

$$X_{j|k}^{(3)} = a_0 + a_1 X_k^{(3)}, \quad (2)$$

i.e. the value of $X_j^{*,(3)}$ predicted from $X_k^{(3)}$ for minimizing measurement error. Its residual variance is $\tau_{j|k}^2 = s_j^2(1 - \rho_{jk}^2)$, and the total error variance with respect to $X_j^{*,(3)}$ is $v_{j|k}^2 = \sigma_j^2 + \tau_{j|k}^2$.

The statistically optimal combination of the direct measurement $X_j^{(3)}$ and the indirect measurement $X_{j|k}^{(3)}$ for assessing $X_j^{*,(3)}$ is the inverse-variance estimate

$$\hat{X}_j^{*,(3)} = w_1 X_j^{(3)} + w_2 X_{j|k}^{(3)}, \quad w_1 = \frac{v_{j|k}^2}{\sigma_j^2 + v_{j|k}^2}, \quad w_2 = \frac{\sigma_j^2}{\sigma_j^2 + v_{j|k}^2}. \quad (3)$$

For providing an answer based on this estimate, the LLM ideally should compare $\hat{X}_j^{*,(3)}$ to the reference midpoint $X_{j,\text{ref}} = (X_j^{(1)} + X_j^{(2)})/2$, similar to a regression model

$$P\left(Y_{jk}^{(e)} = 2 \mid X_j^{(3)}, X_k^{(3)}\right) = h\left(\beta_s \cdot (\hat{X}_j^{*,(3)} - X_{j,\text{ref}})\right) \quad (4)$$

$$= h\left(\beta_{0,jk}^{(e)} + \beta_{1,jk}^{(e)} X_j^{(3)} + \beta_{2,jk}^{(e)} X_k^{(3)}\right) \quad (5)$$

with $h(\eta) = 1/(1 + \exp(-\eta))$, and scaling parameter β_s . Expanding (5) using (2) and (3) shows that $\beta_{1,jk}^{(e)} = \beta_s w_1$ and $\beta_{2,jk}^{(e)} = \beta_s w_2 a_1 = \beta_s w_2 \rho_{jk} \frac{s_j}{s_k}$, hence

$$\frac{\beta_{2,jk}^{(e)}}{\beta_{1,jk}^{(e)}} = \frac{w_2}{w_1} \frac{s_j}{s_k} \rho_{jk}, \quad (6)$$

tying ρ_{jk} to the fitted logistic coefficients $\beta_{1,jk}^{(e)}$ and $\beta_{2,jk}^{(e)}$ through their slope ratio.

2.3 Correlation estimation

Symmetric estimator. The directional relation in (6) depends not only on the correlation ρ_{jk} , but also on nuisance terms tied to variable scaling and relative cue weighting. Using the alternative question version, which flips the role of X_j and X_k , we obtain an estimate of ρ_{kj} . We can exploit two symmetry properties: first, the true correlation is symmetric, $\rho_{jk} = \rho_{kj}$, so both question versions target the same quantity; second, reversing the query exchanges the roles of the two variables and of the corresponding evidence channels. Under this paired-query symmetry, the s_j/s_k scaling cancels exactly and the remaining directional asymmetry is reduced in the product of the two slope ratios

$$\frac{\hat{\beta}_{2,jk}^{(e)}}{\hat{\beta}_{1,jk}^{(e)}} \cdot \frac{\hat{\beta}_{2,kj}^{(e)}}{\hat{\beta}_{1,kj}^{(e)}} \approx \left(\rho_{jk}^{(e)}\right)^2. \quad (7)$$

We recover $\hat{\rho}_{jk}^{(e)}$ from this product by taking the square root and assigning the sign indicated by the fitted slope ratios.

Uncertainty. The surrogate model fit returns a covariance matrix for the fitted coefficients. We propagate this uncertainty through the slope ratios and the symmetric estimator using the delta method, yielding a standard error $\hat{\sigma}_{\rho,jk}^{(e)}$ for each pair and environment. These standard errors enter the ICP stage.

2.4 Invariant causal prediction

Environment-specific correlations. Each environment e specifies a vector of implied patient population means $\mu^{(e)}$ and yields a set of elicited pairwise correlation estimates. Collecting these estimates across environments lets us ask which conditional relationships remain stable across subpopulation shifts, in the spirit of ICP’s observational heterogeneity framing [Peters et al., 2016].

Invariance testing. For a target X_t and a set of candidate predictors $\mathcal{C} \subseteq \mathcal{X} \setminus \{X_t\}$, ICP [Peters et al., 2016] tests subsets $S \subseteq \mathcal{C}$ for stability of the regression of X_t on S across environments. If S contains the direct causes of X_t and the conditional mechanism is stable, these regression slopes should remain invariant. Spurious predictors, by contrast, can change their apparent explanatory power as the marginal means shift. For a given (t, S) pair, let $\hat{R}_{SS}^{(e)}$ denote the estimated $|S| \times |S|$ predictor–predictor correlation matrix and $\hat{r}_{S,t}^{(e)}$ the vector of estimated predictor–target correlations in environment e . We then compute the environment-specific standardised OLS slopes as $\hat{\beta}_{t,S}^{(e)} = (\hat{R}_{SS}^{(e)})^{-1} \hat{r}_{S,t}^{(e)}$. This is the standard OLS formula in the standardised (unit-variance, zero-mean) setting, applied directly to the elicited correlation estimates without any raw data. Uncertainty in $\hat{\beta}_{t,S}^{(e)}$ is propagated from $\hat{\sigma}_{\rho,jk}^{(e)}$ via the delta method, yielding precision matrices $\hat{\Lambda}_{t,S}^{(e)} = [\text{Var}(\hat{\beta}_{t,S}^{(e)})]^{-1}$. We test joint invariance across all m environments via the Wald statistic:

$$W_{t,S} = \sum_{e=1}^m \left(\hat{\beta}_{t,S}^{(e)} - \hat{\beta}_R\right)^\top \hat{\Lambda}_{t,S}^{(e)} \left(\hat{\beta}_{t,S}^{(e)} - \hat{\beta}_R\right), \quad (8)$$

where $\hat{\beta}_R = \left(\sum_e \hat{\Lambda}_{t,S}^{(e)}\right)^{-1} \sum_e \hat{\Lambda}_{t,S}^{(e)} \hat{\beta}_{t,S}^{(e)}$ is the precision-weighted common slope under the null. Under H_0 , $W_{t,S} \sim \chi_{(m-1)|S|}^2$; we accept S as invariant for target t if $p > \alpha$. After testing all subsets $S \subseteq \mathcal{C}$, we retain the variables contained in the intersection of all accepted sets. A variable is retained only if it cannot be excluded from *any* invariant set, making the estimate conservative by design. Repeating this for each target yields a conservative set of candidate parent links.

3 Experiments

Applications. We apply our method to two clinical domains: COPD (pneumology) and MS (neurology). The full variable list is given in Appendix B, grouped by measurement modality. All variables are expressed as z-scores (zero mean, unit variance), which puts them on a common scale despite different units and ranges. For lung function markers in COPD this matches common reporting practice and corrects for age, sex, and height.

Setup. We use OpenAI’s open-weight model gpt-oss-120b and, for the model-size comparison, gpt-oss-20b [OpenAI, 2025]. Both models are distributed under the Apache 2.0 license, subject to the gpt-oss usage policy. Prompts establish a domain-specific expert persona (pneumologist for COPD, neurologist for MS), instruct the model to consider missing values, note that measurements tend to be correlated, and require a binary choice between Patients 1 and 2. We specify environments in the prompt as a short textual description followed by the mean values of selected variables. Unless stated otherwise, no environment is provided.

All triplet experiments use a common dense Cartesian query grid. The core range around the center is extended symmetrically by a small margin of 0.4 and sampled in increments of 0.2, yielding an effective span of ± 1.4 on each axis. Patients 1 and 2 are placed symmetrically around the reference, with $X_j^{(1)} = X_{j,\text{ref}} - 0.5$ and $X_j^{(2)} = X_{j,\text{ref}} + 0.5$. The $X_j^{(3)}$ axis is centered at $X_{j,\text{ref}}$ (default 0 unless explicitly varied), while $X_k^{(3)}$ is centered at 0. Per grid point, we collect 3 binary triplet decisions and extend to at most 6 only if the initial responses are not unanimous. We then aggregate the patient counts and fit a binomial GLM in `statsmodels` [Seabold and Perktold, 2010] by iteratively reweighted least squares.

ICP. For ICP, we use a bipartite design: prompted environments shift a small set of clinically motivated input variables, and the selected variables serve as candidate targets. This avoids testing links within the same modality and focuses the analysis on plausible predictor–outcome directions. Each environment is stated explicitly in the prompt through a short clinical description together with the mean z-score values of the shifted variables. Three environments are defined per application; their descriptions and mean z-score configurations are shown in Table 1.

4 Results

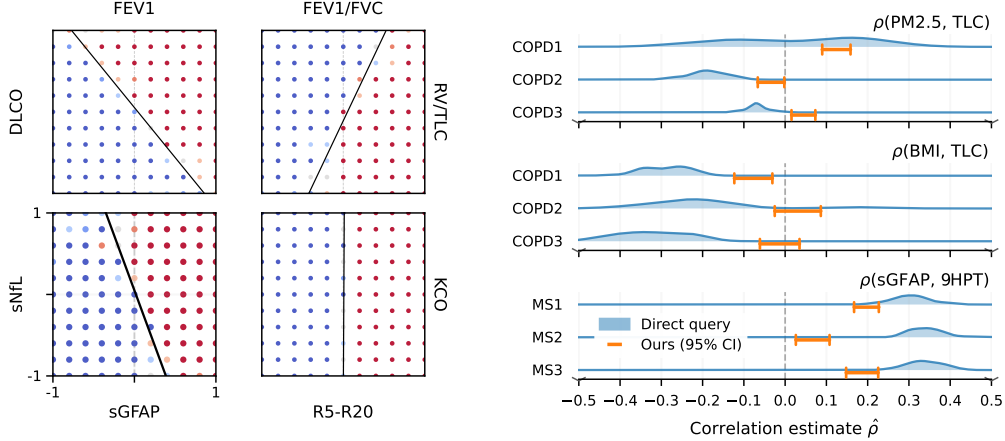
4.1 Recovered correlations

The surrogate decision model fits well. Figure 1a shows the binary LLM response fractions over the queried Patient-3 value grid for four representative variable pairs. Full directed answer-grid matrices for all COPD and MS variable pairs are provided in Appendix C. The empirical response surfaces are smooth and monotone, and the $p = 0.5$ decision boundaries estimated by logistic regression fit the decisions in all cases. The boundary slopes are consistent with the expected sign of the correlation: for positively correlated pairs (e.g. FEV1 and DLCO), the decision boundary has a negative slope—a high value of $X_k^{(3)}$ shifts the decision boundary leftward, as expected when the two variables co-vary positively. The decision surfaces confirm that the decision pattern of the LLM is well described by the surrogate model of Section 2.2, providing empirical support for the elicitation procedure.

Clinical plausibility. Table 2 reports the estimated pairwise correlations $\hat{\rho}$. The implied correlations are clinically plausible and show clearer structure in COPD than in MS. In COPD, the strongest associations lie within measurement modalities: the spirometry variables (FEV1, FEV1/FVC,

Table 1: ICP environments for both applications. Each environment is described by a clinical scenario and the z-score means of the input variables (standardised z-scores).

	<i>Description</i>	sNfL	sGFAP	T1BHV
MS1	The patients are from a relapsing-remitting MS cohort with recent clinical relapses and evidence of active focal white matter inflammation.	+1.5	0.0	-0.5
MS2	The patients are from a progressive MS cohort with diffuse neuroinflammation and predominant grey matter involvement, without recent clinical relapses.	+0.5	+1.5	-0.3
MS3	The patients are from a long-standing MS cohort with high accumulated structural lesion burden and currently low inflammatory activity.	-0.5	-0.5	+1.5
	<i>Description</i>	pack-years	PM2.5	BMI
COPD1	The patients are from a COPD outpatient clinic with a long history of cigarette smoking and typical urban air quality exposure.	+1.5	0.0	0.0
COPD2	The patients are urban residents with no significant smoking history, chronically exposed to elevated ambient fine particulate matter (PM2.5).	-0.5	+1.5	-0.2
COPD3	The patients are from a rural area with clean air and no significant smoking history, recruited from an obesity clinic.	-0.5	-0.8	+1.5



(a) Triplet decision surfaces.

(b) Direct queries and triplet estimates.

Figure 1: Main extracted associations. (a) Answer-grid response fractions with surrogate decision boundaries. Axes are labelled by the clinical variable names and correspond to the queried Patient-3 values of the two variables in each panel. Blue indicates Patient 1, red indicates Patient 2 was chosen. (b) Direct-query distributions and triplet 95 % CIs.

FEF25-75) form a tight block ($\hat{\rho} \approx 0.68-0.73$), as do DLCO and KCO ($\hat{\rho} = 0.68$), whereas oscillometry variables (R5-R20, X5) are less aligned with the others, consistent with oscillometry capturing airway mechanics complementary to conventional spirometry and diffusion testing [Peng et al., 2025]. The signs of key pairs also match established physiology: FEV1/FVC is negatively associated with RV/TLC ($\hat{\rho} = -0.48$) and TLC ($\hat{\rho} = -0.55$), in line with airflow obstruction, air trapping, and hyperinflation in COPD [Alter et al., 2020], while DLCO and TLC are positively correlated ($\hat{\rho} = 0.75$), consistent with the known relation between diffusion capacity and structural lung damage, though this relation can vary by phenotype [Devalla et al., 2024]. In MS, correlations are weaker overall. The largest values occur in a few established pairs, such as T25FW-T2-LV ($\hat{\rho} = 0.40$), T25FW-9HPT ($\hat{\rho} = 0.33$), and sNfL-sGFAP ($\hat{\rho} = 0.38$), whereas most fluid-biomarker-to-clinical-scale pairs remain at or below 0.25. One plausible explanation is that cross-modality associations in MS are represented less strongly in the model, perhaps because the relevant literature is sparser or more heterogeneous than in COPD. SDMT is particularly weakly related to the other variables, including lesion volumes, which is consistent with its use as a measure

Table 2: Estimated pairwise correlations for COPD and MS. Lower-left triangle: COPD. Upper-right triangle: MS. Cell color encodes the estimated correlation (orange: negative, blue: positive).

(a)	sNfL	sGFAP	EDSS	SDMT	T25FW	9HPT	T2-LV	T1-BHV	(b)
FEV1		0.38	0.23	-0.04	0.32	0.25	0.34	0.18	sNfL
FEV1/FVC	0.69		0.16	-0.05	0.21	0.16	0.21	0.16	sGFAP
FEF25-75	0.68	0.73		-0.08	0.22	0.16	0.17	0.16	EDSS
R5-R20	-0.16	-0.20	-0.11		-0.13	-0.02	-0.16	-0.15	SDMT
X5	0.20	0.28	0.27	0.02		0.33	0.40	0.32	T25FW
DLCO	0.72	0.67	0.40	-0.04	0.17		0.19	0.12	9HPT
KCO	0.41	0.51	0.31	0.01	0.15	0.68		0.33	T2-LV
TLC	0.55	-0.55	0.42	0.27	0.16	0.75	-0.09		T1-BHV
RV/TLC	-0.21	-0.48	-0.24	0.29	-0.02	-0.16	-0.15	0.43	
	FEV1/ FVC	FEF25- 75	R5- R20	X5	DLCO	KCO	TLC	RV/ TLC	

of cognitive processing speed and with the only moderate association reported between cognitive performance and white-matter lesion burden in MS [Morrow et al., 2025, Mollison et al., 2017].

4.2 Invariant causal prediction

Table 3 reports the ICP p -values for all non-empty subsets of {pack-years, PM2.5, BMI} as candidate parents for each lung function target (COPD) and {sNfL, sGFAP, T1-black-hole-volume} as candidate parents of the four clinical performance scales (MS). Because ICP is conservative by design—a variable is accepted as a causal parent only if it cannot be excluded from any invariant set—the method frequently returns an empty parent set (denoted —), which should be interpreted as “no robust causal link detected” rather than evidence of no causal relationship.

COPD. Three links survive the intersection: pack-years as a parent of DLCO; PM2.5 as a parent of TLC; and BMI as a parent of R5-R20. The pack-years \rightarrow DLCO link is clinically plausible given the established association between smoking exposure, emphysema, and reduced diffusion capacity [Devalia et al., 2024]. The PM2.5 \rightarrow TLC link is more tentative, but it is directionally consistent with broader evidence linking particulate air pollution to reduced lung function and increased COPD risk [Wang et al., 2025]. The BMI \rightarrow R5-R20 link is also plausible, as oscillometry studies report higher respiratory impedance in obesity [Holtz et al., 2023]. Notably, FEV1/FVC has no accepted parent under ICP despite its clear clinical relation to smoking exposure, illustrating the conservative nature of the procedure.

MS. T1-black-hole-volume (T1-BHV) as a parent of EDSS, and sGFAP as a parent of 9HPT are identified as potential associations.

The T1-BHV \rightarrow EDSS link is consistent with meta-analytic evidence that MRI lesion burden, including T1 lesion volume, is associated with disability in MS [Mirrosayyeb et al., 2024]. The sGFAP \rightarrow 9HPT link remains exploratory, although higher sGFAP has been associated with relapse-independent disability accrual using a composite outcome that includes 9HPT [Rosenstein et al., 2024].

4.3 Validation and sensitivity analyses

Comparison with direct queries. Figure 1b compares the distributions obtained by asking the LLM directly for Pearson correlations (blue kernel density estimates, KDE, based on 50 repetitions) with the estimates from our triplet method (orange 95% CIs). Direct-query responses are much more dispersed, with standard deviations typically in the range 0.1–0.3, whereas the triplet-based confidence intervals are narrower; for $\hat{\rho}_{\text{PM2.5}, \text{TLC}}$, the direct-query distribution is even bimodal, with one positive and one negative peak. They are also less sensitive to prompted environments: the distributions overlap substantially across environments for most variable pairs, while the triplet

pack-years	COPD							MS						
	PM2.5	BMI	FEV1/FVC	RV/TLC	TLC	DLCO	R5-R20	sNFL	sGFAP	TIBHV	EDSS	SDMT	T25FW	9HPT
○	○	●	.000	.989	.004	.000	.056	○	○	●	.579	.631	.000	.000
○	●	○	.002	.000	.052	.000	.002	○	●	○	.048	.987	.000	.539
●	○	○	.003	.982	.038	.720	.048	●	○	○	.006	.830	.026	.000
○	●	●	.000	.010	.001	.000	.000	○	●	●	.183	.927	.000	.001
●	○	●	.000	.983	.004	.000	.003	●	○	●	.052	.848	.000	.000
●	●	○	.000	.002	.061	.000	.015	●	●	○	.001	.965	.000	.002
●	●	●	.000	.077	.006	.000	.001	●	●	●	.014	.958	.000	.000
<i>parents</i>			—	—	PM2.5	pack-years	BMI	<i>parents</i>		TIBHV	—	—	sGFAP	

Table 3: ICP p-values for COPD and MS targets. Filled circles indicate included candidate parents; open circles indicate excluded ones. **Bold** entries are rejected at $p < 0.05$.

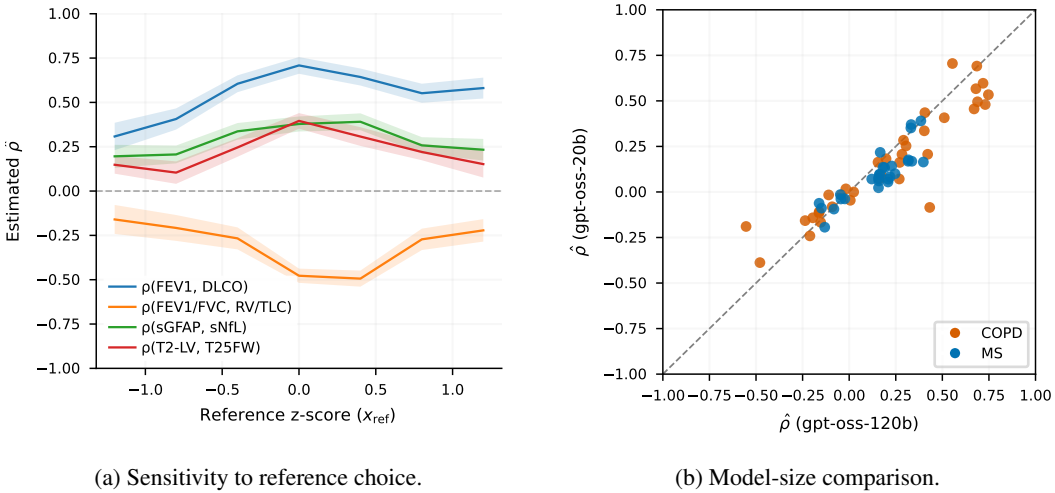


Figure 2: Robustness checks. (a) Sensitivity to the reference value $X_{j,\text{ref}}$ for the queried first variable. (b) Model-size comparison of pairwise $\hat{\rho}$ estimates.

estimates vary more strongly, as required for ICP. Taken together, these patterns suggest that triplet-based correlation estimation is less noisy than direct queries, especially when it comes to discerning differences across environments.

Reference choice. Figure 2a shows how $\hat{\rho}$ varies as a function of the reference value $X_{j,\text{ref}}$ for selected variable pairs. Estimates are stable in the central range ($|X_{j,\text{ref}}| \lesssim 1$) and tend to shrink toward zero in the tails, as expected when the anchor and reference patients become more similar and implied differences are harder to distinguish. One exception is the FEV1–DLCO pair in COPD, which remains elevated even at positive $X_{j,\text{ref}} \approx 1$.

Model size. Figure 2b compares pairwise $\hat{\rho}$ estimates from the large model (gpt-oss-120b, horizontal axis) and the smaller model (gpt-oss-20b, vertical axis) across both applications. Most points lie close to the diagonal, indicating that both models recover a similar relative correlation structure across variable pairs. The gpt-oss-20b estimates are, however, slightly smaller in absolute magnitude, suggesting that the smaller model has internalized the correlation structure less strongly even though the overall association pattern remains similar.

5 Related Work

LLMs as sources of causal knowledge. Some authors queried models directly about causal relations and compared the answers with known graphs or benchmark tasks [Long et al., 2022, Jin et al., 2024, 2023, Zhou et al., 2024, Zečević et al., 2023]. Others used LLM judgments as priors, constraints, or refinements for statistical causal discovery, rather than as complete discovery procedures [Long et al., 2023, Ban et al., 2023, 2025, Darvari et al., 2024, Takayama et al., 2025]. Wan et al. [2025] survey this literature and distinguish direct inference, prior-knowledge integration, and post-hoc refinement. Most of this work elicits knowledge through explicit statements about edges, directions, or causal relevance. We instead recover dependence structure via comparison questions that do not rely on the quality of quantitative statements from LLMs and apply invariant causal prediction only as a second step [Peters et al., 2016].

Knowledge probing and behavioral elicitation. The LAMA benchmark tested whether a model can recover knowledge-base triples from cloze queries [Petroni et al., 2019], and later surveys organized a broad set of related probing methods and datasets [Youssef et al., 2023]. Follow-up work showed that the answer depends strongly on the prompt used to elicit the fact [Shin et al., 2020]. Biomedical variants extend this setting to clinical and scientific relations, where multi-token entities, long-tailed vocabularies, and many-to-many relations make probing harder [Sung et al., 2021, Meng et al., 2022b, Yao et al., 2023]. These studies mostly targeted discrete facts such as entity–relation triples. Closer to our setting, Requeima et al. [2024] elicited numerical predictive distributions from LLMs conditioned on natural-language descriptions and numerical context. Instead of asking the model directly, we infer continuous associations using triplet-style comparisons, which have been used to recover similarity structure from qualitative judgments [Vankadara et al., 2023] and to test whether clinical embeddings agree with expert similarity judgments [Kabus et al., 2026].

Probing and mechanistic interpretability. Probing classifiers can reveal whether representations contain linguistic, factual, spatial, temporal, or truth-related information [Belinkov, 2022, Gurnee and Tegmark, 2024, Marks and Tegmark, 2024, Mallen et al., 2024]. However, encoded information need not be used by the model in the behavior of interest. This distinction has motivated stronger causal tests, including amnesic probing, mediation analysis, activation patching, and model editing [Elazar et al., 2021, Vig et al., 2020, Meng et al., 2022a, Conmy et al., 2023, Lindsey et al., 2025]. These methods can provide mechanistic evidence, but they require access to internal activations and often assume that the relevant computation can be localized. We instead study the model behaviorally, using controlled prompts and observed choices rather than internal activations.

6 Conclusion

We introduced a behavioral framework for extracting association structure from LLMs using structured triplet comparisons. The method turns binary similarity judgments into pairwise correlation estimates without requiring access to model internals, uses prompted subpopulation shifts to compare these estimates across environments and applies ICP as a conservative filter for candidate parent links. In COPD and MS, the recovered correlations were stable and clinically interpretable, with a stronger and more coherent signal in COPD than in MS. Compared with direct correlation queries, the triplet-based estimates were less dispersed and more sensitive to prompted environment shifts, which is important for downstream invariance testing. Additional robustness checks showed stable estimates over central reference choices and broadly consistent association structure across model sizes. These results suggest that structured comparison queries can expose meaningful association structure represented in LLMs.

Several limitations qualify this interpretation. Most notably, the method recovers model-implied rather than empirical clinical associations. Moreover, although the surrogate model fits the observed triplet decisions well, the translation from fitted slopes to correlation estimates still depends on the relational assumptions underlying the estimator and may not capture non-linear internal structure. Finally, the empirical study is limited to two clinical domains, a modest variable set, and a small set of models. Within these limits, the proposed framework provides an exploratory tool for probing association structure in LLMs.

Acknowledgments and Disclosure of Funding

Funded by the Deutsche Forschungsgemeinschaft (DFG, German Research Foundation) – Project-ID 499552394 – SFB 1597.

References

- Peter Alter, Jan Orszag, Christoph Kellerer, Kathrin Kahnert, Tobias Speicher, Henrik Watz, Robert Bals, Tobias Welte, Claus Vogelmeier, and Rudolf A. Jörres. Prediction of air trapping or pulmonary hyperinflation by forced spirometry in COPD patients: Results from COSYCONET. *ERJ Open Research*, 6(3):00092–2020, 2020. doi: 10.1183/23120541.00092-2020. URL <https://doi.org/10.1183/23120541.00092-2020>.
- Taiyu Ban, Lyuzhou Chen, Derui Lyu, Xiangyu Wang, and Huanhuan Chen. Causal structure learning supervised by large language model, 2023. URL <https://arxiv.org/abs/2311.11689>. arXiv preprint arXiv:2311.11689.
- Taiyu Ban, Lyuzhou Chen, Derui Lyu, Xiangyu Wang, Qinrui Zhu, Qiang Tu, and Huanhuan Chen. Integrating large language model for improved causal discovery. *IEEE Transactions on Artificial Intelligence*, pages 1–13, 2025. doi: 10.1109/TAI.2025.3560927.
- Yonatan Belinkov. Probing classifiers: promises, shortcomings, and advances. *Computational Linguistics*, 48(1):207–219, 2022. doi: 10.1162/coli.a.00422.
- Peter G. Brodeur, Thomas A. Buckley, Zahir Kanjee, Ethan Goh, Evelyn Bin Ling, Priyank Jain, Stephanie Cabral, Raja-Elie Abdunour, Adrian D. Haimovich, Jason A. Freed, Andrew Olson, Daniel J. Morgan, Jason Hom, Robert Gallo, Liam G. McCoy, Haadi Mombini, Christopher Lucas, Misha Fotoohi, Matthew Gwiazdon, Daniele Restifo, Daniel Restrepo, Eric Horvitz, Jonathan Chen, Arjun K. Manrai, and Adam Rodman. Performance of a large language model on the reasoning tasks of a physician. *Science*, 392(6797):524–527, 2026. doi: 10.1126/science.adz4433. URL <https://www.science.org/doi/10.1126/science.adz4433>.
- Arthur Conmy, Augustine N. Mavor-Parker, Aengus Lynch, Stefan Heimersheim, and Adrià Garriga-Alonso. Towards automated circuit discovery for mechanistic interpretability, October 2023. URL <https://arxiv.org/abs/2304.14997>. arXiv preprint arXiv:2304.14997.
- Victor-Alexandru Darvari, Stephen Hailes, and Mirco Musolesi. Large language models are effective priors for causal graph discovery, 2024. URL <https://arxiv.org/abs/2405.13551>. arXiv preprint arXiv:2405.13551.
- Lokesh Devalla, Bhalchandra Ghewade, Ulhas S. Jadhav, and Srinivasulareddy Annareddy. Resolving the complexity: A comprehensive review on carbon monoxide diffusion capacity in chronic obstructive pulmonary disease patients. *Cureus*, 16(2):e53492, 2024. doi: 10.7759/cureus.53492. URL <https://doi.org/10.7759/cureus.53492>.
- Yanai Elazar, Shauli Ravfogel, Alon Jacovi, and Yoav Goldberg. Amnesic probing: behavioral explanation with amnesic counterfactuals. *Transactions of the Association for Computational Linguistics*, 9:160–175, 2021. doi: 10.1162/tacl.a.00359.
- Wes Gurnee and Max Tegmark. Language models represent space and time. In *The Twelfth International Conference on Learning Representations*, 2024. URL https://proceedings.iclr.cc/paper_files/paper/2024/hash/0a6059857ae5c82ea9726ee9282a7145-Abstract-Conference.html.
- Mayara Holtz, Laura Perossi, Juliana Perossi, Daniele Oliveira dos Santos, Hugo Celso Dutra de Souza, and Ada Clarice Gastaldi. Respiratory system impedance in different decubitus evaluated by impulse oscillometry in individuals with obesity. *PLOS ONE*, 18(3):e0281780, 2023. doi: 10.1371/journal.pone.0281780. URL <https://doi.org/10.1371/journal.pone.0281780>.
- Ziwei Ji, Nayeon Lee, Rita Frieske, Tiezheng Yu, Dan Su, Yan Xu, Etsuko Ishii, Yejin Bang, Delong Chen, Wenliang Dai, Ho Shu Chan, Andrea Madotto, and Pascale Fung. Survey of hallucination in natural language generation. *ACM Computing Surveys*, 55(12):1–38, December 2023. ISSN 0360-0300, 1557-7341. doi: 10.1145/3571730.

- Zhijing Jin, Yuen Chen, Felix Leeb, Luigi Gresele, Ojasv Kamal, Zhiheng Lyu, Kevin Blin, Fernando Gonzalez Adauto, Max Kleiman-Weiner, Mrinmaya Sachan, and Bernhard Schölkopf. CLadder: assessing causal reasoning in language models. In *Advances in Neural Information Processing Systems*, volume 36, 2023. URL https://proceedings.neurips.cc/paper_files/paper/2023/hash/631bb9434d718ea309af82566347d607-Abstract-Conference.html.
- Zhijing Jin, Jiarui Liu, Zhiheng Lyu, Spencer Poff, Mrinmaya Sachan, Rada Mihalcea, Mona Diab, and Bernhard Schölkopf. Can large language models infer causation from correlation? In *The Twelfth International Conference on Learning Representations*, 2024. URL <https://openreview.net/forum?id=vqIH00bdqL>.
- Fabian Kabus, Julia Hindel, Jelena Bratulić, Meropi Karakioulaki, Ayush Gupta, Cristina Has, Thomas Brox, Abhinav Valada, and Harald Binder. Assessing multimodal chronic wound embeddings with expert triplet agreement, April 2026. URL <https://arxiv.org/abs/2603.29376>. arXiv preprint arXiv:2603.29376.
- Jack Lindsey, Wes Gurnee, Emmanuel Ameisen, Brian Chen, Adam Pearce, Nicholas L. Turner, Craig Citro, David Abrahams, Shan Carter, Basil Hosmer, Jonathan Marcus, Michael Sklar, Adly Templeton, Trenton Bricken, Callum McDougall, Hoagy Cunningham, Thomas Henighan, Adam Jermyn, Andy Jones, Andrew Persic, Zhenyi Qi, T. Ben Thompson, Sam Zimmerman, Kelley Rivoire, Thomas Conerly, Chris Olah, and Joshua Batson. On the biology of a large language model. *Transformer Circuits Thread*, 2025.
- Stephanie Long, Tibor Schuster, and Alexandre Piché. Can large language models build causal graphs? In *Workshop on Causal Machine Learning for Real-World Impact at NeurIPS 2022*, 2022. URL <https://neurips.cc/virtual/2022/61740>.
- Stephanie Long, Alexandre Piché, Valentina Zantedeschi, Tibor Schuster, and Alexandre Drouin. Causal discovery with language models as imperfect experts. In *ICML 2023 Workshop on Structured Probabilistic Inference & Generative Modeling*, 2023. URL <https://icml.cc/virtual/2023/28078>.
- Alex Mallen, Madeline Brumley, Julia Kharchenko, and Nora Belrose. Eliciting latent knowledge from “quirky” language models. In *The First Conference on Language Modeling*, 2024. URL <https://openreview.net/forum?id=nGCMLATBit>.
- Samuel Marks and Max Tegmark. The geometry of truth: emergent linear structure in large language model representations of true/false datasets. In *The First Conference on Language Modeling*, 2024. URL <https://openreview.net/forum?id=aaJyHYjjsk>.
- Kevin Meng, David Bau, Alex Andonian, and Yonatan Belinkov. Locating and editing factual associations in GPT. In *Advances in Neural Information Processing Systems*, volume 35, 2022a. URL https://proceedings.neurips.cc/paper_files/paper/2022/hash/6f1d43d5a82a37e89b0665b33bf3a182-Abstract-Conference.html.
- Zaiqiao Meng, Fangyu Liu, Ehsan Shareghi, Yixuan Su, Charlotte Collins, and Nigel Collier. Rewire-then-probe: a contrastive recipe for probing biomedical knowledge of pre-trained language models. In *Proceedings of the 60th Annual Meeting of the Association for Computational Linguistics (Volume 1: Long Papers)*, pages 4798–4810. Association for Computational Linguistics, May 2022b. doi: 10.18653/v1/2022.acl-long.329.
- Omid Mirmosayyeb, Mohammad Yazdan Panah, Yousef Mokary, Mohammad Mohammadi, Elham Moases Ghaffary, Vahid Shaygannejad, Bianca Weinstock-Guttman, Robert Zivadinov, and Dejan Jakimovski. Neuroimaging markers and disability scales in multiple sclerosis: A systematic review and meta-analysis. *PLOS ONE*, 19(12):e0312421, 2024. doi: 10.1371/journal.pone.0312421. URL <https://doi.org/10.1371/journal.pone.0312421>.
- Daisy Mollison, Robin Sellar, Mark Bastin, Denis Mollison, Siddharthan Chandran, Joanna Wardlaw, and Peter Connick. The clinico-radiological paradox of cognitive function and MRI burden of white matter lesions in people with multiple sclerosis: A systematic review and meta-analysis. *PLOS ONE*, 12(5):e0177727, 2017. doi: 10.1371/journal.pone.0177727. URL <https://doi.org/10.1371/journal.pone.0177727>.

- Sarah A. Morrow, Marina Everest, David Beniamen, and Heather Rosehart. The influence of manual dexterity on processing speed assessment in multiple sclerosis: A comparison of the PST and oral SDMT. *Multiple Sclerosis and Related Disorders*, 104:106799, 2025. doi: 10.1016/j.msard.2025.106799. URL <https://doi.org/10.1016/j.msard.2025.106799>.
- OpenAI. Introducing gpt-oss. <https://openai.com/index/introducing-gpt-oss/>, August 2025. OpenAI product announcement and model overview.
- Junjie Peng, Xiaohua Li, Hong Zhou, Tao Wang, Xiaoou Li, and Lei Chen. Clinical value of impulse oscillometry in chronic obstructive pulmonary disease: A systematic review and meta-analysis. *Respiration*, 104(2):100–109, 2025. doi: 10.1159/000541633. URL <https://doi.org/10.1159/000541633>.
- Jonas Peters, Peter Bühlmann, and Nicolai Meinshausen. Causal inference by using invariant prediction: identification and confidence intervals. *Journal of the Royal Statistical Society Series B: Statistical Methodology*, 78(5):947–1012, November 2016. ISSN 1369-7412. doi: 10.1111/rssb.12167.
- Fabio Petroni, Tim Rocktäschel, Sebastian Riedel, Patrick Lewis, Anton Bakhtin, Yuxiang Wu, and Alexander Miller. Language models as knowledge bases? In *Proceedings of the 2019 Conference on Empirical Methods in Natural Language Processing and the 9th International Joint Conference on Natural Language Processing (EMNLP-IJCNLP)*, pages 2463–2473, Hong Kong, China, 2019. Association for Computational Linguistics. doi: 10.18653/v1/D19-1250.
- Pouya Pezeshkpour and Estevam Hruschka. Large language models sensitivity to the order of options in multiple-choice questions. In *Findings of the Association for Computational Linguistics: NAACL 2024*, pages 2006–2017. Association for Computational Linguistics, 2024. doi: 10.18653/v1/2024.findings-naacl.130.
- James Requeima, John Bronskill, Dami Choi, Richard E. Turner, and David Duvenaud. LLM processes: numerical predictive distributions conditioned on natural language. In *Advances in Neural Information Processing Systems*, volume 37, 2024. URL https://proceedings.neurips.cc/paper_files/paper/2024/hash/c5ec22711f3a4a2f4a0a8ffd92167190-Abstract-Conference.html.
- Igal Rosenstein, Anna Nordin, Hemin Sabir, Clas Malmeström, Kaj Blennow, Markus Axelsson, and Lenka Novakova. Association of serum glial fibrillary acidic protein with progression independent of relapse activity in multiple sclerosis. *Journal of Neurology*, 271:4412–4422, 2024. doi: 10.1007/s00415-024-12389-y. URL <https://doi.org/10.1007/s00415-024-12389-y>.
- Skipper Seabold and Josef Perktold. Statsmodels: Econometric and statistical modeling with python. In *Proceedings of the 9th Python in Science Conference*, pages 92–96, 2010. doi: 10.25080/Majora-92bf1922-011. URL <https://proceedings.scipy.org/articles/Majora-92bf1922-011>.
- Mrinank Sharma, Meg Tong, Tomasz Korbak, David Duvenaud, Amanda Askell, Samuel R. Bowman, Newton Cheng, Esin Durmus, Zac Hatfield-Dodds, Scott R. Johnston, Shauna Kravec, Timothy Maxwell, Sam McCandlish, Kamal Ndousse, Oliver Rausch, Nicholas Schiefer, Da Yan, Miranda Zhang, and Ethan Perez. Towards understanding sycophancy in language models. In *The Twelfth International Conference on Learning Representations*, 2024. URL https://proceedings.iclr.cc/paper_files/paper/2024/hash/0105f7972202c1d4fb817da9f21a9663-Abstract-Conference.html.
- Taylor Shin, Yasaman Razeghi, Robert L. Logan Iv, Eric Wallace, and Sameer Singh. AutoPrompt: eliciting knowledge from language models with automatically generated prompts. In *Proceedings of the 2020 Conference on Empirical Methods in Natural Language Processing (EMNLP)*, pages 4222–4235, Online, 2020. Association for Computational Linguistics. doi: 10.18653/v1/2020.emnlp-main.346.
- Mujeen Sung, Jinhyuk Lee, Sean Yi, Minji Jeon, Sungdong Kim, and Jaewoo Kang. Can language models be biomedical knowledge bases? In *Proceedings of the 2021 Conference on Empirical Methods in Natural Language Processing*, pages 4723–4734, Online and Punta Cana, Dominican Republic, 2021. Association for Computational Linguistics. doi: 10.18653/v1/2021.emnlp-main.388.

- Patrick Suppes, David M. Krantz, R. Duncan Luce, and Amos Tversky. *Foundations of measurement: Geometrical, threshold, and probabilistic representations*. Academic Press, 1989. ISBN 978-0-12-425402-2. doi: 10.1016/C2009-0-21665-5. URL <https://www.sciencedirect.com/book/monograph/9780124254022/foundations-of-measurement>.
- Masayuki Takayama, Tadahisa Okuda, Thong Pham, Tatsuyoshi Ikenoue, Shingo Fukuma, Shohei Shimizu, and Akiyoshi Sannai. Integrating large language models in causal discovery: a statistical causal approach. *Transactions on Machine Learning Research*, 2025. URL <https://openreview.net/forum?id=Reh1S8rxfh>.
- Leena Chennuru Vankadara, Michael Lohaus, Siavash Haghiri, Faiz Ul Wahab, and Ulrike von Luxburg. Insights into ordinal embedding algorithms: a systematic evaluation. *Journal of Machine Learning Research*, 24(191):1–83, 2023.
- Jesse Vig, Sebastian Gehrmann, Yonatan Belinkov, Sharon Qian, Daniel Nevo, Yaron Singer, and Stuart Shieber. Investigating gender bias in language models using causal mediation analysis. In *Advances in Neural Information Processing Systems*, volume 33, pages 12388–12401. Curran Associates, Inc., 2020.
- Guangya Wan, Yunsheng Lu, Yuqi Wu, Mengxuan Hu, and Sheng Li. Large language models for causal discovery: current landscape and future directions. In *Proceedings of the Thirty-Fourth International Joint Conference on Artificial Intelligence*, pages 10687–10695, 2025. doi: 10.24963/ijcai.2025/1186.
- Tinggui Wang, Mengdan Liang, Xiaoying Ye, Xiaoxiao Huang, Hanbing Chen, Xiongkun He, Mengying Xie, Xiaowei Xie, Xiannuan Jiang, Zhehui Chen, Baosong Xie, Yiming Zeng, and Xiaoxu Xie. Ambient air pollution exposure, mediating biomarkers and risk of COPD: A cohort study and meta-analysis. *European Respiratory Review*, 34(177):250055, 2025. doi: 10.1183/16000617.0055-2025. URL <https://doi.org/10.1183/16000617.0055-2025>.
- Zonghai Yao, Yi Cao, Zhichao Yang, and Hong Yu. Context variance evaluation of pretrained language models for prompt-based biomedical knowledge probing. *AMIA Joint Summits on Translational Science Proceedings*, pages 592–601, 2023. URL <https://pubmed.ncbi.nlm.nih.gov/37350903/>.
- Paul Youssef, Osman Alperen Koraş, Meijie Li, Jörg Schlötterer, and Christin Seifert. Give me the facts! A survey on factual knowledge probing in pre-trained language models. In *Findings of the Association for Computational Linguistics: EMNLP 2023*, pages 15588–15605. Association for Computational Linguistics, 2023. doi: 10.18653/v1/2023.findings-emnlp.1043.
- Matej Zečević, Moritz Willig, Devendra Singh Dhami, and Kristian Kersting. Causal parrots: large language models may talk causality but are not causal. *Transactions on Machine Learning Research*, 2023. URL <https://openreview.net/forum?id=tv46tCzs83>.
- Yu Zhou, Xingyu Wu, Beicheng Huang, Jibin Wu, Liang Feng, and Kay Chen Tan. CausalBench: a comprehensive benchmark for causal learning capability of LLMs, 2024. URL <https://arxiv.org/abs/2404.06349>. arXiv preprint arXiv:2404.06349.

A Prompt Templates

This appendix shows the abstract prompt templates used in the experiments. We replace implementation-specific fields by placeholders such as [expert persona], [environment description], and the variable names X_j and X_k , while keeping the substantive wording of the prompts unchanged. Here [environment description] stands for the full environment specification: the textual cohort description together with the mean values of the shifted variables, as listed in Table 1. All numeric values are rendered with one decimal place.

Triplet comparison prompt.

```
[expert persona]
All values are population-normalized z-scores: 0.0 = population
mean, 1.0 = one population standard deviation.
[environment description]

Patient 1:  $X_j$  = [value],  $X_k$  = missing
Patient 2:  $X_j$  = [value],  $X_k$  = missing
Patient 3:  $X_j$  = [value],  $X_k$  = [value]

Infer the missing  $X_k$  values for Patients 1 and 2 from their observed
 $X_j$  values.
Be mindful that clinical variables and biomarkers tend to be highly
correlated.
Then choose which patient (1 or 2) is more similar to Patient 3.

Respond with exactly one line containing only:
1
or
2
```

Direct correlation query prompt.

```
[expert persona]

What is the Pearson correlation coefficient between  $X_j$  and  $X_k$  in
the relevant patient population?
[environment description]

Reason through this carefully. Consider the physiological or
clinical relationship between the two variables, draw on specific
studies, cohorts, or reference ranges you are aware of, and discuss
any factors that might strengthen or attenuate the association.
Weigh conflicting evidence if it exists.

On the very last line of your response, write exactly (and nothing
else):
correlation: X.XX
```

Persona texts.

Table 4: Prompt persona texts.

Domain	Persona text
COPD	You are a pneumologist specialized in obstructive and restrictive lung disease.
MS	You are a neurologist specialized in multiple sclerosis and demyelinating disease.

B Variable Reference

Table 5: Variables and descriptions for COPD and MS.

	<i>Modality</i>	Variable	Description
COPD	<i>Spirometry</i>	FEV1	Forced expiratory volume in 1 s.
		FEV1/FVC	Ratio of FEV1 to FVC; obstructive ratio.
		FEF25-75	Mean forced expiratory flow, 25%–75% of FVC.
	<i>Oscillometry</i>	R5-R20	Frequency-dependent resistance (5 Hz – 20 Hz).
		X5	Respiratory system reactance at 5 Hz.
	<i>Diffusion</i>	DLCO	Diffusing capacity for carbon monoxide.
		KCO	Transfer coefficient (DLCO / alveolar volume).
<i>Plethysmography</i>	TLC	Total lung capacity.	
	RV/TLC	Residual volume fraction of total lung capacity.	
MS	<i>Fluid Biomarkers</i>	sNFL	Neurofilament light chain; neuroaxonal damage.
		sGFAP	Glial fibrillary acidic protein; astrocyte damage.
	<i>Clinical Scales</i>	EDSS	Expanded Disability Status Scale.
		SDMT	Symbol Digit Modalities Test; processing speed.
		T25FW	Timed 25-Foot Walk; ambulation.
		9HPT	9-Hole Peg Test; manual dexterity.
	<i>MRI Lesions</i>	T2-lesion-volume	T2-hyperintense white matter lesion volume.
		T1-black-hole-volume	T1-hypointense lesion volume; axonal loss.

C Full Answer Grids

Figures 3 and 4 show the full directed answer-grid matrices for all COPD and MS variable pairs.

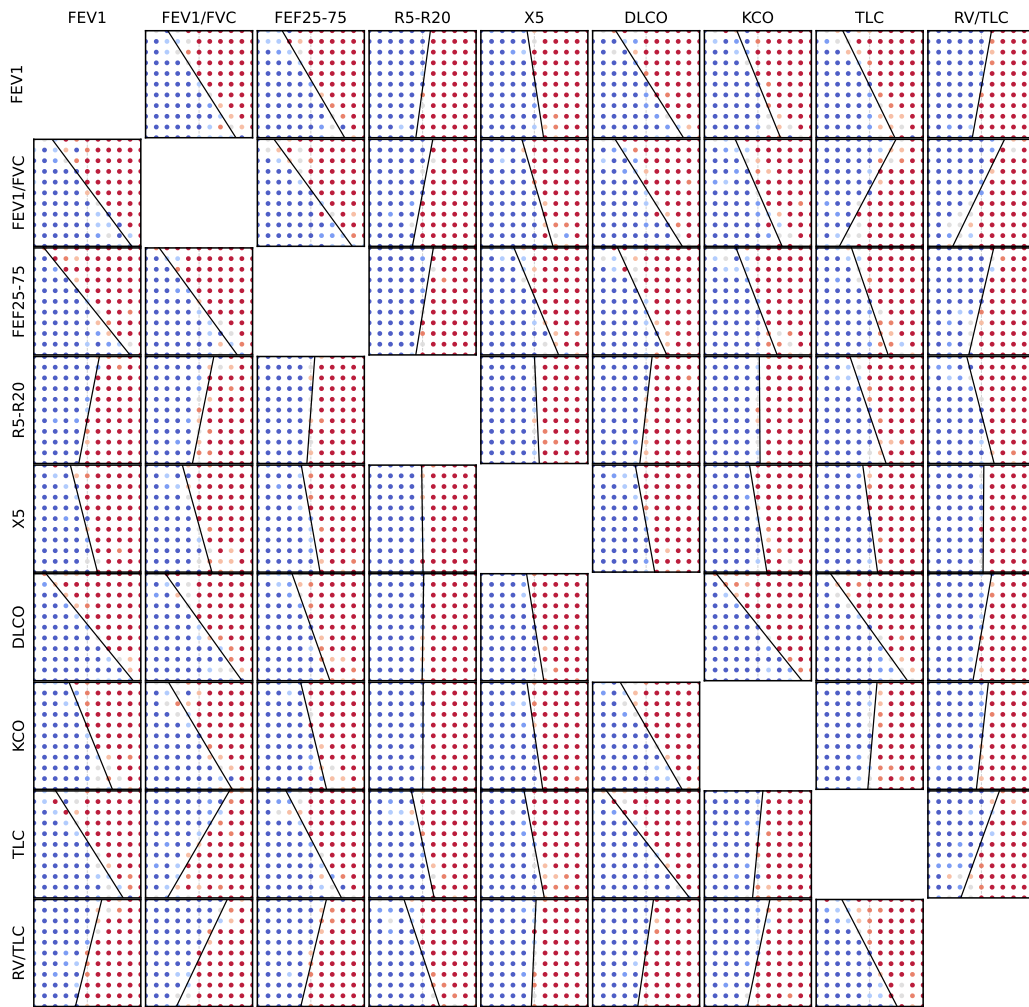


Figure 3: Full COPD answer-grid matrix.

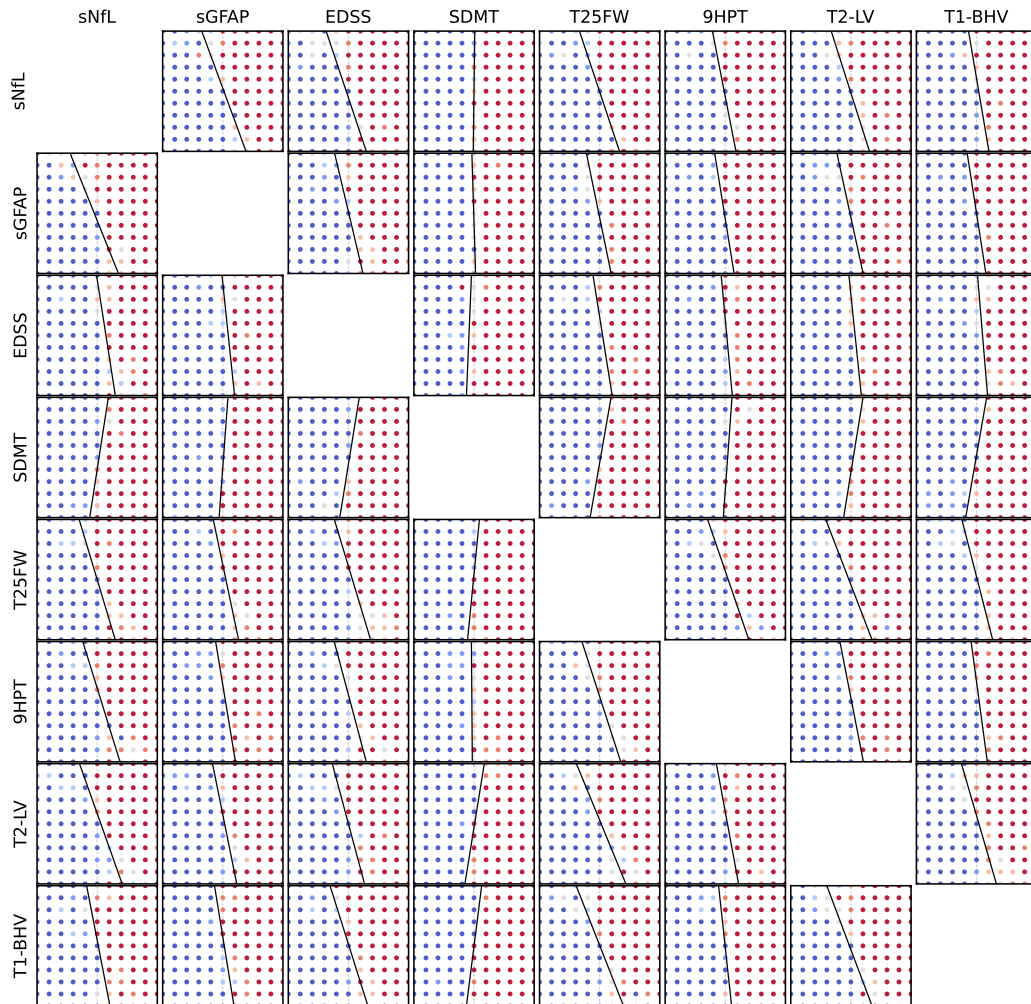


Figure 4: Full MS answer-grid matrix.

D Compute Resources

Table 6 summarizes the number of LLM requests required by the main analysis blocks underlying the reported results. The experiments were run on our local cluster. For the Slurm jobs underlying the reported artifacts, we reserved 8 CPU cores, 48 GB host memory, and 1 GPU. The model server ran via vLLM on a single NVIDIA H100 GPU with 95,830 MiB VRAM; the compute node class uses AMD EPYC 9454 processors. After warm-up, average throughput was approximately 9 requests per second. During method development, some analyses were rerun multiple times, so total development-time request counts were higher than the final counts reported here, although caching reduced repeated inference costs.

Table 6: LLM request counts for the main analysis blocks.

Analysis block	Supported artifacts	Requests
Pairwise correlation (gpt-oss-120b)	Table 2 and Figure 1a	52,545
Pairwise correlation (gpt-oss-20b)	Figure 2b	53,400
ICP analysis	Table 3 and Figure 1b	78,960
Reference-value sweeps	Figure 2a	23,871